Value of local offshore renewable resource diversity for network hosting capacity

Citation for published version:
Sun, W, Harrison, G & Harrison, S 2020, 'Value of local offshore renewable resource diversity for network hosting capacity', *Energies*, vol. 13, no. 22, 5913. https://doi.org/10.3390/en13225913

Digital Object Identifier (DOI):
10.3390/en13225913

Link:
Link to publication record in Edinburgh Research Explorer

Document Version:
Peer reviewed version

Published In:
Energies

energies

MDPI

Article

Value of local offshore renewable resource diversity for network hosting capacity

Wei Sun [1], Sam Harrison [2] and Gareth P. Harrison [1,*]

[1] School of Engineering, University of Edinburgh, Mayfield Road, Edinburgh EH9 3DW, UK; W.Sun@ed.ac.uk
[2] Department of Electronic and Electrical Engineering, University of Strathclyde, Glasgow G1 1XQ, sam.harrison@strath.ac.uk
* Correspondence: Gareth.Harrison@ed.ac.uk

Received: date; Accepted: date; Published: date

Abstract: It is imperative to increase the connectable capacity (i.e. hosting capacity) of distributed generation in order to decarbonise electricity distribution networks. Hybrid generation that exploits complementarity in resource characteristics among different renewable types potentially provides value for minimising technical constraints and increasing the effective use of the network. Tidal, wave and wind energy are prominent offshore renewable energy sources. It is of importance to explore their potential complementarity for increasing network integration. In this work, the novel introduction of these distinct offshore renewable resources into hosting capacity evaluation enables the quantification of the benefits of various resource combinations. A scenario reduction technique is adapted to effectively consider variation of these renewables in an AC optimal power flow-based NLP optimisation model. Moreover, the beneficial impact of Active Network Management (ANM) on enhancing the renewable complementarity is also investigated. The combination of complementary hybrid generation and ANM, specifically where the maxima of the generation profiles rarely co-occur with each other and with the demand minimum, is found to make the best use of the network components.

Keywords: hosting capacity; electricity distribution network; tidal; wave; offshore wind; optimisation

1. Introduction

The rapid deployment of renewable generation in the last two decades has seen the introduction of new power sources on the distribution network. Previously, power flowed strictly from supply to demand but distributed generators (DG) have transformed the structure of distribution networks. The installed capacity of DG on UK networks reached 26 GW in 2019, 24% of installed renewable capacity, and is projected to increase to 36% by 2050 [1]. Although the integration of DG has significant benefits in decarbonising the electricity industry [2], it also brings a series of challenges to network operation due to the variability and uncertainty of renewable output. Bi-directional power flow, voltage rise and increased fault level have been identified as key issues that DG poses to network operation [3]. As the share of DG increases, the pressure on network capacity due to voltage rise and reverse power flow will rise. Therefore, there is a critical need to fully utilise the network capacity to connect DG by exploring the potential of different DG configurations and considering new network management techniques. The research on how to locate and size renewable DGs to maximise their overall connectable capacity is often referred to as 'hosting capacity' in the literature [4,5].

Hybrid generation comprising different types of renewable generation offers a potentially valuable route to better balance their output and increase their grid integration [6–8]. The time-varying nature of renewable resources creates less predictable and uncontrollable generation peaks and troughs. Generation peaks which coincide with periods of low demand define the worst-case scenarios that drive voltage rise and increased reverse power flow on distribution networks. Ultimately, these conditions determine the capacity that Distribution Network Operators (DNOs) are willing to connect. If generation is based on resources with different profiles, either resulting from temporal or spatial differences, then individual extreme peaks may be suppressed, and network constraints might be avoided or reduced. A DNO could then connect more capacity.

The complementarity between different renewable resources seems to be highly dependent on the location in which the study is made; however, in general, research has proven that a diversified portfolio of renewables improves their output reliability. Many studies have focused on the analysis of complementarity among wind, PV and hydroelectricity generation to facilitate grid integration. These studies have reported valuable complementarity in different locations and time scales [9–11]. Hoicka et al. investigated wind and solar in Ontario, Canada and found complimentary resources result in less variability of power output [12]. The solar and wind resources around China were modelled using the MERRA-2 reanalysis dataset and the complementarity of wind and PV connected more capacity than individual resources [13]. In [14], the strong temporal synergy of solar and wind resource is found in Australia and their combination increases the use of existing transmission assets. In [15], annual and interannual complementarities among wind, PV and hydropower are explored in Colombia for stable power supply during the annual dry season and the El Nino Sothern Oscillation. The impact of complementarity on small scale hybrid wind-PV systems is studied in [16] and the authors proposed a set of complementarity indices for power supply reliability. The work in [17] found that the joint operation of PV and hydro stations helps to increase PV integration and also raises their profit on the day-ahead market. Halamay et al. also identified the diversification of resources at large scale as a way to reduce utility reserve requirements [18]. The value of local hybrid solar-wind systems is examined in [19] and shows the benefit of the combination of the hybrid generation and the value of selective curtailment of generation.

While the renewable complementarity for increasing grid-integration is an active research field, studies on the complementarity involving both wave and tidal resources are sparse. There are a few studies on combining wind only with wave. The complementarity of wind and wave resources at locations around Europe have been compared, and sites that had two generation profiles with stable behaviour and low correlation were found to reduce the variability of power output to the grid [20]. Similar studies include the evaluation of co-located wind and wave for the US west coast and the UK North Sea [21], Latin America and Europe [22]. These works mainly look at the supply profile of the combined resources but do not consider their feasibility regarding network capacity constraints.

Another popular route for increasing hosting capacity for renewables is through the use of advanced network control schemes [23,24]. Historically, DNOs have connected DG with a 'fit-and-forget' or 'passive control' approach where generator unit capacities are constrained at the planning stage so that when connected they can operate without intervention. This hosting capacity is defined according to often infrequent worst-case scenarios, where low demand coincides with high generation output, making relatively inefficient use of the network. The downside of this approach has been widely recognised and the potential to make better use of the network by using active network management (ANM) techniques has been well articulated. Several different ANM control schemes have been proposed. In a method referred to as co- ordinated voltage control (CVC), on-load tap changers (OLTC) are used to change (lower) the set-point voltage on the secondary side of transformers, mitigating voltage rise [25]. Power factor control (PFC) varies the DG power factor from inductive to capacitive depending on the direction of required voltage control [26,27]. Alternatively, DNOs may reserve the right to reduce power output via active curtailment control (ACC) during periods that stretch the network capabilities [28,29]. ANM has been trialled on a distribution network on the Orkney Islands, Scotland with power flow management through ACC used successfully to keep network components within their thermal limits [30]. Optimal power flow (OPF) techniques have been developed to understand how DG affects distribution network operation, the constraints to deployment, and how connectable capacity may be enhanced [31–33]. Multi-period AC OPFs have indicated that ANM schemes (notably ACC, CVC and PFC) increase the capacity of wind generation connected to distribution networks [34].

Summarizing the research gap identified in the existing literature: firstly, regarding complementarity of multiple renewable resources few – if any – consider the complementary potential of offshore wind, wave and tidal energy sources to improve connectable capacity. Secondly, few existing works on resource complementarity explicitly consider the reliable operation of networks in terms of voltage and thermal limits in distribution network. In contrast, this study takes a rigorous approach and thoroughly investigates the complementary benefits of these three offshore renewable resources in alleviating network constraints and increasing the hosting capacity. Moreover, the additional benefits from active network management are also studied in detail. The main contribution of this work can be described as:

1. The novel introduction of three offshore renewable resources – offshore wind, wave and tidal stream – to a hosting capacity study. A multivariate scenario reduction technique is adapted to effectively consider variation and complementarity of renewables over a long time period.
2. The generic AC OPF based hosting capacity model is established to find the simultaneous hosting capacity for various resource combinations considering their complementarity and a suite of ANM control schemes. The hosting capacity problem is formulated as a Nonlinear Optimisation model (NLP) to accurately model voltage and thermal constraints.
3. Comparative analysis is detailed in the case study in Scotland for different configurations of renewable resources and control schemes. This identified which resources combine to offer enhanced hosting capacity and energy delivery and which features constrain the performance of network control schemes.

This paper is structured as follows: Section 2 introduces the optimisation model for hosting capacity analysis. Section 3 introduces the case study and section 4 provides the resource evaluation and hosting capacity analysis and discussion. The conclusion is provided as the last section.

2. AC OPF Model for Hosting Capacity Analysis

An AC OPF based approach is adopted here to model a hosting capacity problem with the objective to maximise the overall connectable capacity of candidate DG located at specified locations across the network. The OPF formulation is widely used to find the optimal control settings for a power network to fulfil its objective function whilst remaining within network limits. An AC solution is preferred as it accounts for active and reactive network components, both of which are known to affect voltage levels, a key constraint to generation on distribution networks. While traditionally used for operational analysis, it has found use in 'planning' analysis such as for hosting capacity analysis where the capacity of generators are optimised [32,34].

The normal AC OPF is extended here to consider multiple resources and multiple time periods. The multi-periodicity grasps the time-varying nature of demand and renewable generation profiles; specifically the need to capture a wide range of conditions requires a large number of time periods (at least a year) at relatively high time resolution (such as hourly). Hybrid generation configurations can easily be analysed using a multi-period approach which account for their differing temporal characteristics. The OPF-based nonlinear optimisation model is implemented in the modeling language AIMMS [35] and solved using the CONOPT 4.0 NLP solver.

Before the formal mathematical description, it is worth explaining how the optimisation operates in simple terms. The model uses the DG production and demand in each time period and determines the resulting set of power flows. As the DG size(s) are increased, the production across all periods will increase, changing the power flows and resulting in higher voltages and larger reverse power flows. Where DG is not actively controlled, the DG(s) capacity will be increased until a voltage or thermal constraint is reached in one or more periods (normally that with maximum production and minimum demand). This defines the hosting capacity.

Where there are ANM controls in place and DG capacity and production increase, voltages and reverse power flows increase. However, where a constraint is reached in a period the optimisation will look to change the control setting (power factor, transformer voltage or curtailment) such that the DG capacity can increase further. Each time period is treated separately but more periods will tend to see changes in control settings as the DG capacity increases. This continues until one or more of the control settings have reached their limit (e.g. power factor limits, transformer voltage limits or maximum curtailment), defining the hosting capacity.

2.1. Objective Function

More formally, the objective function of the optimisation is to maximise the total connectable capacity of potential DGs of different resource types located at specified locations in the network over all considered renewable resources:

$$max \sum_{g\in G} \sum_{r\in R} \; p_{r,g}, \tag{1}$$

where $p_{r,g}$ is the active power capacity of generator g for resource r.

2.2. Network Constraints

The three major constraints that the optimisation is subject to are: (1) active and reactive power balance, (2) voltage limits and (3) power flow limits.

2.2.1. Active and Reactive Nodal Power Balances

The active power balance equations are derived from Kirchhoff's Current Law and define the power flow into and out of each bus:

$$\sum_{l\in L|\beta_l^{1,2}=b} p_{b,m}^L + d_b^p \eta_m = \sum_{g\in G_b} \sum_{r\in R} p_{r,g}\omega_{r,m} + \sum_{x\in X_b} p_{x,m} \tag{2}$$

where $p_{b,m}^L$ is the active power injection into connecting lines L from bus b in period m; η_m is demand in each period expressed relative to peak value d_b^P. $\omega_{r,m}$ is the generator output level for the resource r during period m and is defined as the instantaneous output as a fraction of the maximum/nominal output (i.e. capacity factor), and is determined by the resource characteristics such as wind speed in corresponding periods m. If the bus is connected to external connection x, typically the grid supply point (GSP), any excess or deficit of production is met from exports/imports $p_{x,m}$ from the external network.

The reactive power balance constraints can be derived similarly:

$$\sum_{l\in L|\beta_l^{1,2}=b} q_{b,m}^{\mathrm{L}} + d_b^Q \eta_m = \sum_{g\in G_b} \sum_{r\in R} p_{r,g}\omega_{r,m}\, tan(\phi_{r,g,m}) + \sum_{x\in X_b} q_{x,m} \tag{3}$$

where the reactive power output of DG is calculated based on its power factor angle $\phi_{r,g,m}$.

2.2.2. Voltage Limits

Network bus voltages $V_{b,m}$ over all time periods must be within defined limits described by lower and upper boundaries, V_b^-, V_b^+:

$$V_b^- \le V_{b.m} \le V_b^+ \tag{4}$$

2.2.3. Power Flow Limits

Flow of power through each line and transformer has specified flow limits imposed by the equipment capabilities and described as:

$$\left(f_{l,m}^{(1,2),P}\right)^2 + \left(f_{l,m}^{(1,2),Q}\right)^2 \le (f_l^+)^2 \tag{5}$$

where $f_{l,m}^{(1,2),P}$ and $f_{l,m}^{(1,2),Q}$ are, respectively, the active and reactive flows through line/transformer l and f_l^+ is the apparent power flow limit.

2.3. Active Network Management

ANM schemes are expected to complement the efforts of hybrid generation configurations for maximising DG production. Active network management aims to adapt control settings for network components and DG on an ongoing basis in response to network constraints. Depending on the scheme these define target DG production levels and power factors as well as transformer set-points in each period that serve to allow larger generators and more energy production. The three schemes discussed in the introduction are simulated to investigate their benefit to networks.

2.3.1. Active Curtailment Control

Curtailment control selectively reduces DG active power output in periods when voltage or power flow limits would otherwise be breached, by reducing reverse power flows. In the model, curtailment $p_{r,g,m}^{curt}$ is considered as a variable, applied by the DNO when the network is constrained, that reduces the active power delivered in period m. The resulting power production in period m $(p_{r,g} - p_{r,g,m}^{curt})$ takes the place of the simple generator capacity previously included in Eq. 2:

$$\sum_{l\in L|\beta_l^{1,2}=b} p_{b,m}^L + d_b^p \eta_m = \sum_{g\in G_b}\sum_{r\in R}(p_{r,g} - p_{r,g,m}^{curt})\omega_{r,m} + \sum_{x\in X_b} p_{x,m} \tag{6}$$

with a similar replacement required for Eq. 3. The amount of curtailment applied to each renewable DG is limited by its full potential output in the corresponding period:

$$p_{r,g,m}^{curt} \le p_{r,g}\omega_{r,m} \tag{7}$$

To ensure a realistic level of curtailment that a developer might agree to, the level of curtailment of each DG is restricted by the curtailment factor $\lambda_{r,g}^{curt}$, a proportion of the total potential energy generation over the full study period M (e.g. over a whole year) as a global limit:

$$\sum_{m\in M} p_{r,g,m}^{curt}\tau_m \le \lambda_{r,g}^{curt}\left[\sum_{m\in M} p_{r,g}\omega_{r,m}\tau_m\right] \tag{8}$$

where τ_m is the duration of period m, e.g. an hour.

2.3.2. Power Factor Control

Power factor control enables local voltage control close to the DG to alleviate voltage constraints. DGs are simulated with the capability to dispatch their power factor $\phi_{g,m}$ from period to period, within the inductive and capacitive limits of the DG (ϕ_g^-, ϕ_g^+):

$$\phi_g^- \le \phi_{g,m} \le \phi_g^+ \tag{9}$$

Making power factor $\phi_{g,m}$ more inductive will tend to reduce reverse power flows and limit voltage rise, enabling larger generators to be connected.

2.3.3. Coordinated Voltage Control

Coordinated voltage control allows the GSP transformer secondary voltage $V_{b_{OLTC,m}}$ to be set to raise or lower overall voltage levels in the network. The secondary voltage is a variable in the model constrained within the range indicated by the transformer tap changer limits (V_{bOLTC}^-, V_{bOLTC}^+):

$$V_{b_{OLTC}}^- \le V_{b_{OLTC,m}} \le V_{b_{OLTC}}^+ \tag{10}$$

In general, setting a lower secondary voltage will tend to allow greater generation by enabling a greater degree of voltage rise relative to the substation.

2.4. Treatment of Long-term Time-series Data

It is important that the full variation of renewable resource and demand over an extended period (e.g. a year) is captured in the analysis, so that the obtained DG capacities satisfy all operational conditions. However, the non-convex nonlinear nature of the hosting capacity optimisation model makes this quite challenging. For example, the direct use of hourly data for one year in the optimisation will generate 8760 operational scenarios to be considered simultaneously, which means a significant number of time-varying variables and corresponding constraints, making the nonlinear optimisation problem laborious or intractable.

To address the computational challenge whilst effectively preserving the temporal interrelationships between resources and demand, scenario reduction is adopted here. The approach uses 'representative' combinations of demand and renewable resource level as inputs, rather than the direct use of full time series. The first step is to discretize the original values, the illustration of which is shown in Figure 1 using the example of demand and wind data. After the discretization, the values are aggregated according to the occurrence of 'similar' periods and allocated into a series of bins covering specific intervals. Such treatment of long-term time-series data was previously detailed in [34], which also showed that discretisation only has a minor impact on accuracy. This paper further develops it to address the 'coincidence' of three different resources (i.e. tidal, wave and wind) and demand, essentially a four dimensional array.

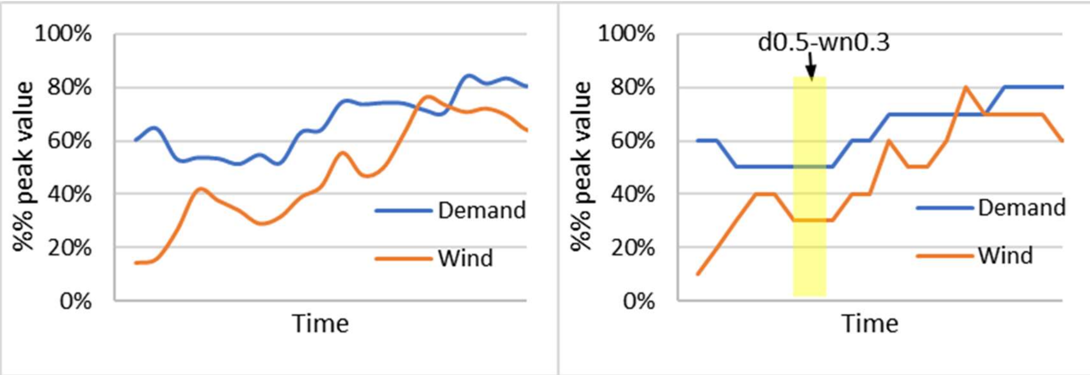

(**a**) (**b**)

Figure 1. (**a**) Normalised hourly demand and wind power time series; (**b**) discretised wind and demand time series. 'd0.5-wn0.3' is the period with demand at 50% of peak and wind at 30% of capacity.

3. Orkney Island Case Study

The case study considers application of the method to a representative location suitable for co-located offshore wind, wave and tidal resources. The resource data relates to part of Orkney off the north coast of Scotland which has a valuable combination of strong winds, an energetic wave climate and sites suitable for tidal stream by virtue of its position between the North Atlantic and the North Sea.

3.1. Resource Evaluation

Three resource profiles with hourly resolution are built from observational and modelled datasets from North Ronaldsay, Orkney using concurrent 2016 data. The location of the data sites is shown in Figure 2. Hourly offshore wind speed (m/s) and wave power density (per metre of wave crest) time series are based on the ECMWF ERA5 reanalysis dataset [36] which has been extensively validated. A tidal current velocity time series (m/s) is built from the FOAM Shelf Seas – Atlantic Margin Model (AMM7) coupled hydrodynamic-ecosystem model [37]. Due to the resolution of the model it slightly under-estimates current velocities so a scaling factor is applied to the tidal profile to raise the 25 highest current velocities to equal the observed local average peak spring velocity [38].

Three representative devices are used to convert the resource time series into production time series. A 1 MW, 18 m rotor diameter SeaGen tidal turbine [39] is chosen to convert tidal energy. The nature of the flow off the tip of North Ronaldsay is thought to be effectively captured by the bi-directional capability of the turbine. A Pelamis wave energy converter, scaled up from 750 kW to 1500 kW as in [40], is chosen due to its wide coverage of energy period and wave height. Although this device is no longer being actively developed for commercialisation, it is well suited to the site characteristics around Orkney and is deemed appropriate to exhibit the benefits of hybrid generation. A generic wind power curve based on a 7.58 MW 127 m diameter direct-drive Enercon E-126 at 80m hub height is used to convert the wind resource. The resulting year-long hourly generation profiles are shown in Figure 3 along with the electricity load profile [40].

Tidal: The SeaGen capacity factor is 27.2%, a product of many hours spent at slack water between energetic flood and ebb flows typical of tidal turbines. The variation of tidal generation is dominated by semi-diurnal and fortnightly cycles determined by celestial orbits.

Wave: The scaled up Pelamis device achieves a capacity factor of 38%, which is comparable with some of the most efficient wave converter locations analysed in a recent study [41]. Figure 3 shows that the wave profile has a strong seasonal variation with calmer summers and more energetic winters.

Wind: Offshore wind generation has the highest capacity factor of the three generator types, reaching 51.2%. Wind exhibits a similar, but less pronounced seasonal distribution to the wave profile. Regular high production (relative to the generator capacity) will increase energy delivered but will also tend to stretch the limits of the network which may affect how wind is handled in the optimisation.

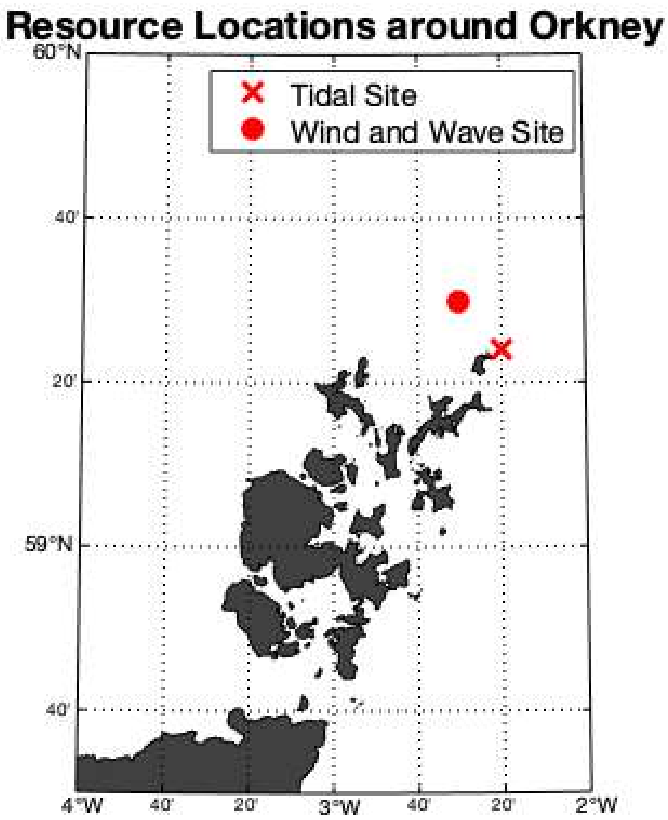

Figure 2. Resource sites co-located off North Ronaldsay, Orkney. Red markers indicate the location that data was collected from ECMWF ERA5 and FOAM AMM7 datasets for resource profiles.

To investigate the relationship among these generation types, and also between each generation type and load, their correlation coefficients are provided in Table 1. The peak cross-correlation coefficients and their associated lags are also calculated and given in Table 2.

A low correlation between the tidal profile and demand or other generation profiles is attributed to the misalignment of the production timescales with those for the others. Independence from other profiles could either support or suppress the inclusion of tidal generation in a hybrid configuration. Generation unrelated to the demand profile will cause frequent imbalance between generation and demand and tend to limit connectable capacity, as peaks of the two are not expected to co-occur. However, an opposite and beneficial impact can be expected with two unrelated generators, where the isolation of peaks reduces the overall generation peak and reduces the strain on the network. Wind and wave profiles are related by moderately high correlation (Table 1) with maximum cross-correlation occurring with a six-hour lag relative to the wind profile (Table 2). Large lags between wind and wave were attributed in [24] to sites where the mechanisms driving wind and wave variation were isolated by the Atlantic fetch, seemingly appropriate for the site north of Orkney, and potentially describing the results. [42] also noted the benefit that lower correlation and higher peak lags offer hybrid generation configurations in the form of smoother power output with fewer zero hours. Table 1 and 2 suggest the wave and wind resource off North Ronaldsay may complement one another more than the same two resources analysed at other selected locations in Europe.

Table 1. Correlation coefficients (r) between load and generation profiles.

	Load	Tidal	Wave	Wind
Load	1.000	0.027	0.220	0.090
Tidal	-	1.000	-0.013	-0.017
Wave	-	-	1.000	0.595
Wind	-	-	-	1.000

Table 2. Peak cross-correlation coefficient (**xR**) and the associated lag (**xL** (**hrs**)) at which it occurs between generation profiles. Data is presented in the table in the form: **xR/xL**, where **xL** is positive when the signal on the left of the table lags the signal above. Cross correlations associated with a lag of more than 24 hours are thought to lack physical meaning.

	Tidal	Wave	Wind
Tidal	1.000/0	0.479/-277	0.494/-252
Wave	-	1.000/0	0.864/6
Wind	-	-	1.000/0

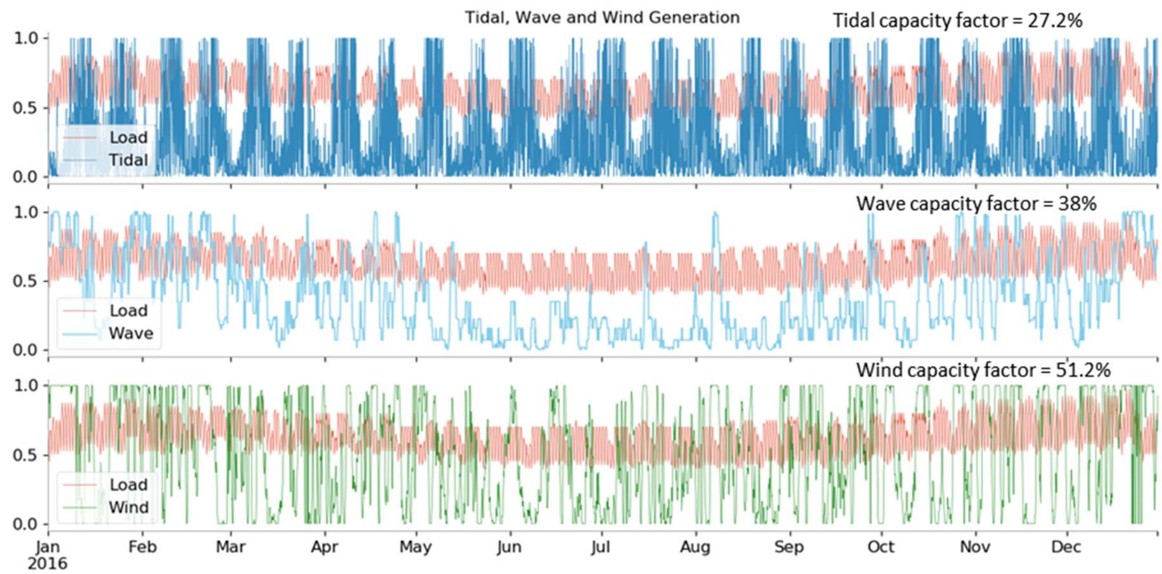

Figure 3. Generation profiles for resources located off North Ronaldsay for the year 2016. Generation is plotted as a proportion of maximum output. The load profile for the studied network is also plotted as a proportion of maximum demand (red dashed line).

3.2. Network Description

A typical but deliberately simple rural distribution network [43], outlined in Figure 4, is used to analyse the co-located offshore renewable resources. This is not the actual network constructed in Orkney but is used to enable comparison with earlier work using the same network [44]. The buses at the end of each feeder offer DG connection sites at bus C and bus E. The two sites have the potential to harness any of the three resources considered in the optimisation due to the proximity of each resource's high energy regions.

Each bus is connected with local load, the sum of which has a maximum of 15.1 MW and minimum of 5.5 MW. The network is supplied by one 110/38 kV transformer at the grid supply point (GSP). Line and transformer information is given in Table 3. Voltage variation is limited to the range of ±10%, and the transformer OLTC voltage target is fixed at 1.078 per unit when an ANM scheme is not considered. During the consideration of CVC, the tap changing potential at the GSP is +5/-15%. Power factor control is limited to power factors between ±0.9. The curtailment limit is set at 10% of the total potential energy output of each generation type throughout the study period.

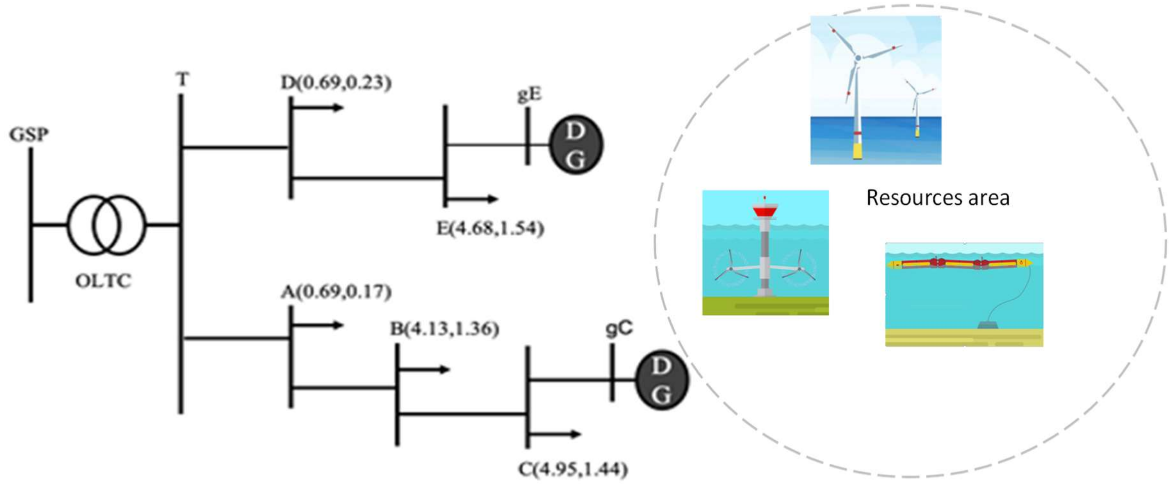

Figure 4. Rural distribution network and local resource area during maximum loading. The maximum real and reactive powers are included with the bus label i.e. bus A: A (P, Q).

Table 3. Line and transformer parameters (resistance R, reactance X and maximum apparent power flow limit S_{max}) for the distribution network. All data are given as per unit values on a 100 MVA base.

Line	R	X	S_{max}
GSP - T	-	0.2500	0.3150
T - A	0.0296	0.0863	0.3817
A - B	0.5941	0.6244	0.1975
B - C	0.3875	0.4072	0.1975
T - D	1.126	1.193	0.3817
D - E	0.1550	0.1629	0.1975
C - gC	0.1292	0.1357	0.1975
E - gE	0.1292	0.1357	0.1975

3.3. Resource-Demand Coincidence

In their original state, the demand and generation profiles take the form of four time-series each with 8760 hourly steps. The NLP optimisation program cannot directly account for such a large dataset, particularly with more than one bus location. Instead, the scenario reduction technique in Section 2.4 is applied to use the duration of coinciding demand-generation levels as input for the NLP to reduce the computational burden.

The hourly demand and generation data of each resource are fitted to various operating state bins, in percentage of its peak value, centered around 10% steps from 0 to 100%. Demand never falls into a bin lower than 40%, so only 7 of the 11 load states are considered. Periods can then be defined as every combination of demand and generation operating state that occurs in the dataset. The duration of the period is simply the number of hourly occurrences. This unique combination is observed throughout the year.

A total of seven different resource configurations are considered in generating the profile of coincident hours: single resources, hybrids of any two, and all three resources together. Figure 5 depicts the bivariate distributions of demand with each individual resource and their coincident hours. For brevity and also due to difficulty with visualization, the tri- and quadri-variate distributions are not shown for each case. However, the 'worst-case' scenarios are listed in Table 4 which show the periods of high generation (100%) and low demand (40%) which are particularly restrictive to the connection of DG capacity. The coincident hours of these show that the occurrence of worst case periods varies considerably. Single resource tidal and wind cases exhibit the highest coincident hours, wave exhibits somewhat less and none of the 4 hybrid resource combinations exhibit more 'worst-case' hours than wave alone. This demonstrates that there is potential value in diverse combinations in terms of reducing the frequency of capacity limiting periods.

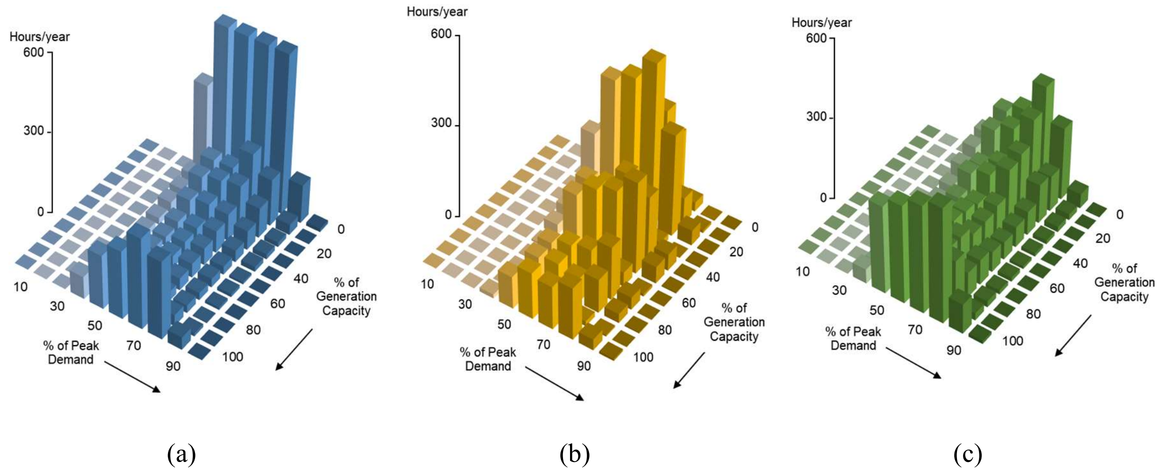

Figure 5. Coincident hours of load and generation states for each offshore renewable. Bins are centered at 10% steps of the peak value of each profile: (**a**) tidal and demand; (**b**) wave and demand; (**c**) wind and demand.

Table 4. Annual duration of worst case scenarios expected to limit the connected capacity for each configuration of generation topology. The level of demand (d), and tidal (t), wave (wv), or wind (wn) generation is indicated as a percentage of its maximum, for example, d04t10 signifies a period with demand at 40% of peak and tidal at 100%.

Configuration	Period	Duration (hours)
Tidal	d04t10	87
Wave	d04wv10	15
Wind	d04wn10	56
Tidal+Wave	d04t09wv10	1
Tidal+Wind	d04t10wn10	6
Wave+Wind	d04wv10wn10	15
Tidal+Wave+Wind	d04t10wv08wn10	1
Tidal+Wave+Wind	d04t09wv10wn10	1

4. Results

Different combinations of resources and control schemes are studied to explore their ability to maximise hosting capacity and the delivered energy. They are grouped into two subsections:

- Single resource cases
- Hybrid generation cases with combinations of two or three resources: tidal+wave, tidal+wind, wave+wind, tidal+wave+wind.

Each resource case is examined subject to six different network control schemes: passive network (i.e. No ANM) or actively managed network with either active curtailment control (ACC), Co-ordinated Voltage Control (CVC) and Power Factor Control (PFC) applied individually or with ACC combined with CVC or PFC.

Table 5 provides the results of hosting capacity for all studied cases and Table 6 is the corresponding delivered energy. To aid comparison, the derived effective capacity factor, as the ratio of actually delivered energy to the amount of energy that would have been produced at full capacity, is given in Table 7.

To investigate the impact of different cases on network operation in terms of voltage and line loading variations, the total hours during the year with *at least* one bus voltage actively constrained by its upper limits are summarized and shown in Figure 6, with equivalent analyses for voltage lower limits, line flow limits and average line loading given in Figures 7-9, respectively. The power injection of DG would generally raise the voltage profiles and could also cause line overloading when the injection largely exceeded local demand. The maximum voltage rise occurs during high generation-low demand periods which ultimately determine the capacities of DG. While the voltages and line loadings are constrained by the optimisation to prevent any limit violation, the frequency of them reaching their limits and the average values over a whole year could indicate the effective use of the network headroom for connecting renewable capacity.

4.1. Hosting Capacity for Single Renewable Type

Table 5.a shows that for all single resource cases in passive networks (i.e. no ANM) the capacity is constrained to the same value due to the same worst case scenario event (maximum generation-minimum demand), irrespective of the duration. There is however difference in the energy delivered (Table 6.a) which reflects the variation in capacity factor of each generation type at the location analysed.

Voltage rise during this scenario is the limiting factor to hosting capacity in this passive network and which occur at the points of connection of the DG (i.e. buses gC and gE). It can be concluded that voltage control schemes would release additional connectable capacity and CVC and PFC control are successful for all renewable types. The increased capacity pushes the voltages in non-worst-case periods towards the upper voltage limits, so the total hours where voltages reach the maximum allowed values increase considerably, as shown in Figure 6.a. Additionally, the large reverse power flows along the feeders result in lines' thermal limits being reached (Figure 8.a) in the lower rated sections between buses A to gC and D to gE with overall loading levels raised considerably (Figure 9.a). The PFC controlled network cases record more hours constrained by voltage and reach the inductive power factor limits (while attempting to lower voltage at the DG buses), but experience fewer periods with constrained lines. CVC is the most successful single ANM scheme in increasing DG capacity and energy delivery due to the highest line usage. The network wide effects of CVC are more effective than the more localised impact of PFC.

Although the ACC cases do not enable as high connection capacity as the previous two control cases, it does distinguish between resource types. By implementing ACC, the sporadic peaky nature of the wave profile allows curtailment to remove its irregular peaks (as its maximum peak only coincides with the low demand for 15 hours, as shown in Table 3) allowing greater capacity than the tidal or wind cases. Curtailment is less effective for both the tidal and wind case which have more regular maximum and other high production states. Despite the 22% extra capacity, the lower capacity factor means wave still delivers 7% less energy (Table 6.a).

Combining ACC with another control scheme makes much more effective use of network capacity with the combination of ACC and CVC showing higher overall capacity and energy delivery than with PFC. The difference is particularly stark with the wave profile, where it is possible to connect almost six times the wave capacity than in the passive case, nearly matching the energy delivery by the equivalent wind case (Table 6.a). The combined control schemes stretch the power flow limits substantially and with PFC in particular, there is very frequent occurrence of upper voltage limits. Figure 7.a shows that lower voltage limits are occasionally met in the tidal and wind cases with ACC and CVC control, because high demand coincides with low generation and the range of the voltage set-point at the GSP OLTC restricts the network capacity. This does not occur with the wave case where maximum demand never coincides with zero generation.

The high overall capacity factor of the wind resource enables the wind cases to deliver the most energy in all cases. The choice of control is highly influential on the wave cases as outlined above and the tidal cases are consistently lower and the scope for capacity increases derived from ACC is lessened by the regular peaks and troughs associated with the resource. Despite differences in capacity and energy delivery among these single resources cases, their effective capacity factors in Table 7.a show the same trend: without ACC it is the same as the capacity factor of the resource; when ACC is involved, it is lower and the percentage reduction from its resource capacity factor is equal to the given curtailment limit, i.e. 10%.

Table 5. Connected generation capacity (MW) for a range of network control configurations. Rows indicate the generation types connected to the network. Columns indicate the network management scheme(s).

		No ANM	CVC	PFC	ACC	ACC CVC	ACC PFC
(a) single resource	Tidal	10.06	38.25	31.34	16.94	47.67	42.12
	Wave	10.06	38.25	31.34	21.37	58.83	52.43
	Wind	10.06	38.25	31.34	17.23	48.19	42.66
(b) hybrid resource	Tidal+Wave	10.78	39.20	32.51	27.30	76.15	67.59
	Tidal+Wind	10.06	38.25	31.34	23.51	67.48	59.40
	Wave+Wind	10.06	38.25	31.34	21.47	58.84	52.46
	Tidal+Wave+Wind	10.78	39.20	32.51	27.30	76.23	67.62

Table 6. Energy delivered (GWh/year) from different resource cases for a range of control configurations.

		No ANM	CVC	PFC	ACC	ACC CVC	ACC PFC
(a) single resource	Tidal	23.94	91.08	74.62	36.30	102.15	90.27
	Wave	33.49	127.40	104.38	64.05	176.34	157.15
	Wind	45.08	171.48	140.51	69.50	194.43	172.13
(b) hybrid resource	Tidal+Wave	29.06	118.85	83.64	72.66	202.11	178.99
	Tidal+Wind	34.96	142.78	80.86	72.46	213.45	187.64
	Wave+Wind	39.53	148.74	105.88	67.56	180.02	159.58
	Tidal+Wave+Wind	29.06	128.59	87.42	72.66	205.97	180.69

Table 7. Effective capacity factor (delivered energy after curtailment) for a range of control configurations.

		No ANM	CVC	PFC	ACC	ACC CVC	ACC PFC
(a) single resource	**Tidal**	27.2%	27.2%	27.2%	24.5%	24.5%	24.5%
	Wave	38.0%	38.0%	38.0%	34.2%	34.2%	34.2%
	Wind	51.2%	51.2%	51.2%	46.1%	46.1%	46.1%
(b) hybrid resource	**Tidal+Wave**	30.8%	34.6%	29.4%	30.4%	30.3%	30.2%
	Tidal+Wind	39.7%	42.6%	29.5%	35.2%	36.1%	36.1%
	Wave+Wind	44.9%	44.4%	38.6%	35.9%	34.9%	34.7%
	Tidal+Wave+Wind	30.8%	37.4%	30.7%	30.4%	30.8%	30.5%

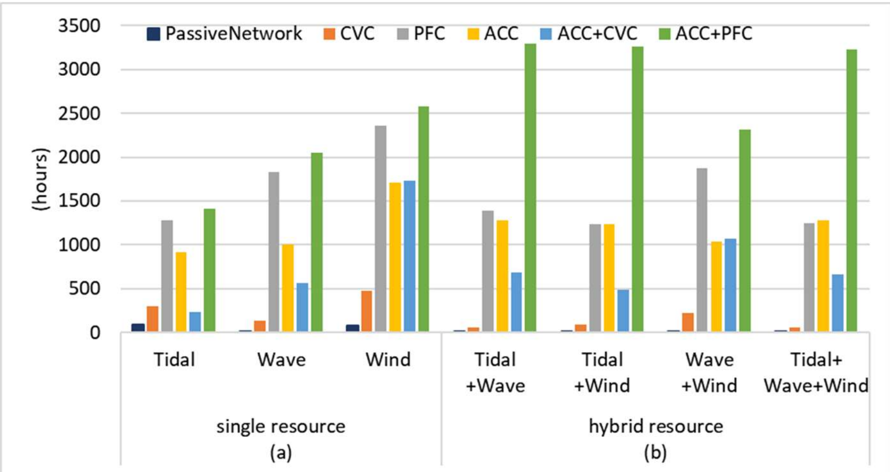

Figure 6. Total hours in the year when at least one bus voltage reaches its upper limits: (**a**) for single resource networks; (**b**) for hybrid resource networks.

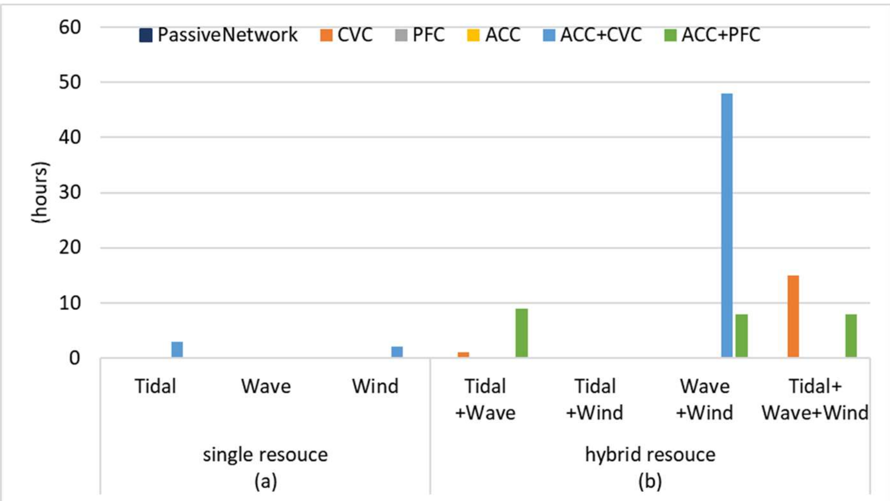

Figure 7. Total hours in the year when at least one bus voltage reaches its lower limits: (**a**) for single resource networks; (**b**) for hybrid resource networks.

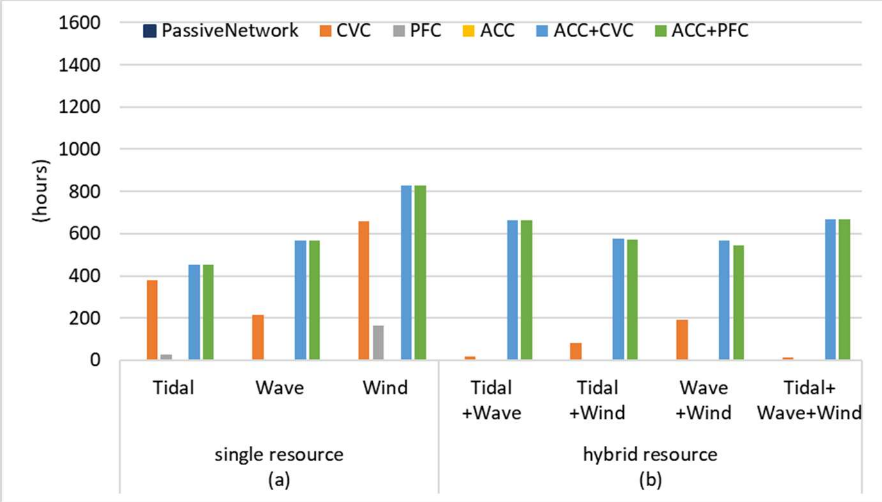

Figure 8. Total hours in the year when the loading of at least one line reaches its full value: (**a**) for single resource networks; (**b**) for hybrid resource networks.

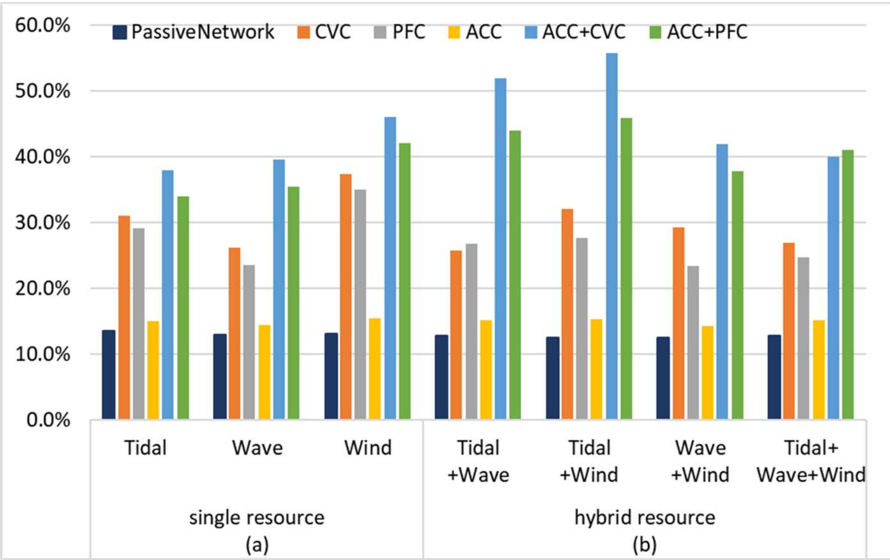

Figure 9. Average line loading in the whole year as percentage of its full value: (**a**) for single resource networks; (**b**) for hybrid resource networks.

4.2. Hosting Capacity for Hybrid Generation

Tables 5.b and 6.b show the corresponding capacity and energy delivery for cases with multiple resources and Figure 10 shows the considerable variation in capacity split between resources in each case. In the passive cases, the tidal+wind and wave+wind combinations have overall capacity that precisely matches that of the individual resources; in both cases the wind represents 52% of the overall capacity suggesting the wind profile has the critical characteristic as far as limiting the hosting capacity. There is a small (~7%) capacity increase from connecting tidal+wave as the joint generation maximum never coincides with minimum demand; here the capacity split is 67% tidal meaning that the effective capacity factor is around 31%. The tidal+wave+wind case records an identical capacity split as no wind is allocated as this would introduce a further constraint due to the coincidence of maximum generation. The energy delivery from each combination is the weighted average of their resource capacity factors and all are lower than wind alone and higher than tidal alone. Overall, the passive network appears to be unable to exploit resource complementarity: neither capacity nor energy delivery fundamentally increases relative to single resources cases.

With CVC and to a lesser extent PFC there are considerable increases in capacity relative to the passive cases delivering higher capacity factors and energy delivery. Both control schemes are again not able to fully exploit resource diversity as overall capacity increases are similar to single resource cases, although the tidal+wave and triple resource cases again have marginally higher capacity (2 to 4%). There is more variation in capacity split between cases. With CVC wind becomes relatively more significant in the tidal+wind case, marginally less in the wave+wind case and does considerably better in the tidal+wind and triple resource cases. Wave improves its share while tidal decreases in all cases. With PFC, tidal becomes more dominant with wind almost disappearing from the tidal+wind case and not featuring in the triple resource case. The network-wide approach of CVC facilitates greater exploitation of wind capacity than the more limited impact of PFC. The hosting capacity of hybrid resources in passive and CVC/PFC hybrid networks is limited by the same constraining factors that limit their single resource counterparts; the effect of CVC is clearly seen in Figure 7.b with the occurrence of the low voltages at the GSP OLTC.

The first major benefit of hybrid generation is seen in the ACC cases. Complementarity is found to support up to 60% increased capacity and energy delivery relative to single resource cases, particularly the tidal+wave case. The worst performing hybrid case (wave+wind) has slightly greater capacity than the highest for single resources (i.e. wave, Table 5.b) and its energy production is around 5% higher (Table 6.b). Interestingly, with the exception of the wave+wind case, all other cases produce more energy than the wind only case, albeit with considerably greater capacities. While the increase in capacity relative to the passive case is lower for ACC than for either CVC or PFC case due to less effective management of voltage constraints, selective curtailment delivers capacities and energy production that are more balanced between resources (Figure 10); wave capacity becomes dominant, particularly when combined with wind.

The combination of control schemes (ACC+CVC, ACC+PFC) facilitates greater exploitation of the complementarity observed between resources. Both sets of cases see a similar pattern of capacity split between resources with very balanced splits except in the triple resource and tidal+wind cases where there is, respectively, little or no wind. The capacity gains over single resource cases is again at most 60% (Table 5.b) with all but the wave+wind cases producing more energy than wind alone (Table 6.b). The most effective is combining ACC with CVC: with ACC suppressing the peaks of the wave profile and CVC managing voltage rise issues, the tidal+wave case makes greater use of network line capacity than any other control configurations, pushing the average line loading closer to its full value (Figure 9.b). With ACC+PFC, voltage limits constrain the network more than other cases in Figure 6 and inductive power factor limits are regularly met as the generators attempt to lower voltages.

While the capacity split between resources, as shown in Figure 10, indicates complex variation between cases, it does allow indicative outcomes regarding complementarity among resource types. The less similar the profiles, the better the complementarity with higher total capacity and a more even split. Despite suggestions that wave and wind complementarity will smooth the power output on useful timescales due to offsets of a number of hours [42], the regular co-occurrence of maximum generation levels here means their complementarity is lower. In the case of wave+wind, considerably more capacity is allocated to wave whose profile sees fewer worst-case periods and benefits more from curtailment at peak output than wind. Alternatively, the combination of the more independent tidal resource with either wave or wind supports higher capacity and a more even allocation between generators due to the lower occurrence of high generation-low demand periods. Despite tidal+wind connecting less capacity than tidal+wave, the large fraction of wind supports the largest energy delivery of any case, almost 5 times more than the passive wind case (Table 5.b).

The cases with full hybrid (tidal+wave+wind) capacity replicate or rise slightly above the best capacity obtained from the two-resource cases. Capacity is mainly allocated to tidal and wave, and a small amount of wind capacity is only seen in the CVC, ACC+CVC and ACC+PFC cases (Figure 10.d). This is because the complementarity between tidal and wave is better than with wind and introducing wind adds undesirable periods of constraints. As a result, in terms of delivered energy, the tidal+wave+wind case is outperformed by a two-resource combination in the ACC + CVC and ACC+PFC cases. Overall, compared with the best performing two-resource cases, there was little benefit seen from a combination of all three resources. Despite differences in capacity and energy delivery, the same trend in constraining factors applies to the tidal+wave+wind case regarding the effectiveness of control configurations: ACC+CVC reaches voltage limits less than ACC+PFC (Figure 6).

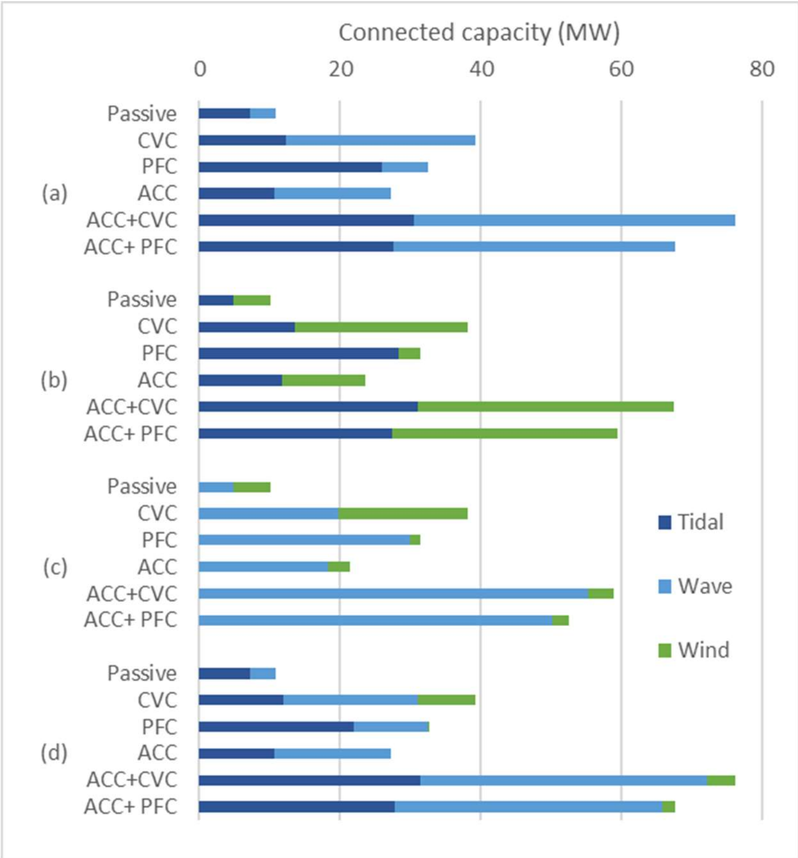

Figure 10. Capacity breakdown by resource type for hybrid cases with actively managed networks: (**a**) tidal+wave; (**b**) tidal+wind; (**c**) wind+wave; (**d**) tidal+wave+wind. Stack colour indicates the capacity of the individual resources.

5. Discussion

As far as we know this is the first analysis to consider these specific resources with regard to hosting capacity analysis and demonstrates some benefit from resource complementarity in terms of exploiting network capacity and energy delivery and very considerable benefits from active network management.

The complementarity level among resource types determines the level of capacity that can be connected. The less similar the profiles are the better. Despite suggestions that wave and wind complementarity will smooth the power output on useful timescales [42], offset from one another by a number of hours, this study finds the regular co-occurrence of both maximum generation levels would reduce the benefit from hybridisation. Instead, the combination of the independent tidal resource with either wave or wind supports higher capacity and energy delivery, due to their fewer occurrence of high generation-low demand periods.

The only comparator analysis is for solar and wind [19], and although the location, networks and specifics of the analysis were different, some qualitative comparison is possible. This showed that solar and wind exhibited greater complementarity and a more significant benefit in terms of additional hosting capacity and energy delivery. Further work looking at a wider portfolio of renewables would therefore be valuable.

While the focus here was very much on network capacity, recognising the value of resource diversity is a matter not just of local diversity in an individual network, but also the effect of geographical diversity as well as the operational and planning impacts on the wider power system.

This takes the value well beyond a view that more capacity is better towards a more nuanced assessment of efficiency in terms of energy per unit of capacity and value for money, particularly given the earlier developmental stage of tidal and wave. The application of this hybridisation involving tidal, wave and offshore wind depends on the development of effective tidal and wave generator arrays. While solar and wind currently offers a more mature alternative, for the best use of hosting capacity, renewable combinations should be based on their complementary characteristics and not simply their current industrial development.

There are a number of qualifications to the results that are worth stating. First, the analysis covers only a year of data, meaning that it does not capture interannual variations in overall resource levels nor the specific timings of each resource which do vary from weather system to weather system. Some difference would be expected should a different year or longer period be used, although the fundamental principles will hold. The framework is well set up to do a longer analysis. Secondly, the resource levels and the statistical relationships between them will vary depending on the location being affected by local geography as well as large scale wind, wave and tidal forcings. It would be valuable to repeat the analysis at other locations to identify if the benefits of complementarity change particularly as the relative level of capacity factors varies. Thirdly, the specific topology of the network, local demand and the control systems will have a considerable impact on the local value of complementarity.

5. Conclusions

In this work, the complementary value of three local offshore renewable resources – tidal, wave and wind – for increasing network hosting capacity is evaluated. A generic AC OPF based hosting capacity model is established to find the maximum connectable capacity for multiple renewable resources. A scenario reduction technique is adapted to effectively consider long-term variation and complementarity of the renewables in the NLP optimisation model.

The novel introduction of three resource types to the hosting capacity evaluation saw a complex picture of increased network utilization through diversity. A second resource tended to increase network hosting capacity and energy delivery but there was little benefit seen from a combination of all three resources arising from co-occurrence of high generation with low demand that could not be fully overcome by active network management. The analysis confirms that traditional passive control schemes make inefficient use of network hosting capacity irrespective of the resource combination. Although all active network control schemes made substantially more effective use of the network, those involving active curtailment exploited coincidence characteristics among demand and multiple renewable types well. Without curtailment the value of complementarity is quite modest for this location although it should be emphasized that additional analysis is warranted to better understand the phenomenon.

In future work, integration options such as energy storage and demand response can be incorporated into the model to further assess the hosting capacity for the offshore renewable resources. Considering that grid integration of variable renewable generation could also cause issues with power quality, fault level and frequency, these technical challenges are worthy of further research.

Author Contributions: Conceptualization, W.S. and G.P.H.; methodology, W.S., S.H. and G.H.; software, S.W.; validation, W.S. and G.P.H; formal analysis, W.S., S.H. and G.P.H.; investigation, W.S., S.H. and G.H.; resources, G.P.H.; data curation, S.W.; writing—original draft preparation, S.H.; writing—review and editing, W.S., S.H. and G.P.H.; visualization, S.H. and W.S.; supervision, W.S. and G.P.H.; project administration, W.S.; funding acquisition, G.P.H. All authors have read and agreed to the published version of the manuscript.

Funding: This research was funded by the Engineering and Physical Sciences Research Council through the EPSRC Centre for Doctoral Training in Wind and Marine Energy Systems (grant number EP/L016680/1) and the EPSRC National Centre for Energy Systems Integration (grant number EP/P001173/1).

Conflicts of Interest: The authors declare no conflict of interest.

References

1. National Grid, E.S.O. Future Energy Scenarios. *National Grid Electricity System Operator: London, UK* **2019**, 1–166.
2. Mehigan, L.; Deane, J.P.; Gallachóir, B.P.Ó.; Bertsch, V. A review of the role of distributed generation (DG) in future electricity systems. *Energy* **2018**, *163*, 822–836, doi:10.1016/j.energy.2018.08.022.
3. Keane, A.; Ochoa, L.F.; Borges, C.L.T.; Ault, G.W.; Alarcon-Rodriguez, A.D.; Currie, R.A.F.; Pilo, F.; Dent, C.; Harrison, G.P. State-of-the-art techniques and challenges ahead for distributed generation planning and optimization. *IEEE Transactions on Power Systems* **2013**, *28*, 1493–1502, doi:10.1109/TPWRS.2012.2214406.
4. Ismael, S.M.; Abdel Aleem, S.H.E.; Abdelaziz, A.Y.; Zobaa, A.F. State-of-the-art of hosting capacity in modern power systems with distributed generation. *Renewable Energy* **2019**, *130*, 1002–1020, doi:10.1016/j.renene.2018.07.008.
5. Mulenga, E.; Bollen, M.H.J.; Etherden, N. A review of hosting capacity quantification methods for photovoltaics in low-voltage distribution grids. *International Journal of Electrical Power and Energy Systems* **2020**, *115*, 105445, doi:10.1016/j.ijepes.2019.105445.
6. Jurasz, J.; Canales, F.A.; Kies, A.; Guezgouz, M.; Beluco, A. A review on the complementarity of renewable energy sources: Concept, metrics, application and future research directions. *Solar Energy* **2020**, *195*, 703–724, doi:10.1016/j.solener.2019.11.087.
7. Han, S.; Zhang, L. na; Liu, Y. qian; Zhang, H.; Yan, J.; Li, L.; Lei, X. hui; Wang, X. Quantitative evaluation method for the complementarity of wind–solar–hydro power and optimization of wind–solar ratio. *Applied Energy* **2019**, *236*, 973–984, doi:10.1016/j.apenergy.2018.12.059.
8. Schindler, D.; Behr, H.D.; Jung, C. On the spatiotemporal variability and potential of complementarity of wind and solar resources. *Energy Conversion and Management* **2020**, *218*, 113016, doi:10.1016/j.enconman.2020.113016.
9. Couto, A.; Estanqueiro, A. Exploring Wind and Solar PV Generation Complementarity to Meet Electricity Demand. *Energies* **2020**, *13*, 4132, doi:10.3390/en13164132.
10. Zhang, H.; Cao, Y.; Zhang, Y.; Terzija, V. Quantitative synergy assessment of regional wind-solar energy resources based on MERRA reanalysis data. *Applied Energy* **2018**, *216*, 172–182, doi:10.1016/j.apenergy.2018.02.094.
11. Viviescas, C.; Lima, L.; Diuana, F.A.; Vasquez, E.; Ludovique, C.; Silva, G.N.; Huback, V.; Magalar, L.; Szklo, A.; Lucena, A.F.P.; et al. Contribution of Variable Renewable Energy to increase energy security in Latin America: Complementarity and climate change impacts on wind and solar resources. *Renewable and Sustainable Energy Reviews* **2019**, *113*, 109232, doi:10.1016/j.rser.2019.06.039.
12. Hoicka, C.E.; Rowlands, I.H. Solar and wind resource complementarity: Advancing options for renewable electricity integration in Ontario, Canada. *Renewable Energy* **2011**, *36*, 97–107, doi:10.1016/j.renene.2010.06.004.
13. Ren, G.; Wan, J.; Liu, J.; Yu, D. Spatial and temporal assessments of complementarity for renewable energy resources in China. *Energy* **2019**, *177*, 262–275, doi:10.1016/j.energy.2019.04.023.
14. Prasad, A.A.; Taylor, R.A.; Kay, M. Assessment of solar and wind resource synergy in Australia. *Applied Energy* **2017**, *190*, 354–367, doi:10.1016/j.apenergy.2016.12.135.
15. Henao, F.; Viteri, J.P.; Rodríguez, Y.; Gómez, J.; Dyner, I. Annual and interannual complementarities of renewable energy sources in Colombia. *Renewable and Sustainable Energy Reviews* **2020**, *134*, 110318, doi:10.1016/j.rser.2020.110318.
16. Jurasz, J.; Beluco, A.; Canales, F.A. The impact of complementarity on power supply reliability of small

scale hybrid energy systems. *Energy* **2018**, *161*, 737–743, doi:10.1016/j.energy.2018.07.182.
17. Jurasz, J.; Kies, A.; Zajac, P. Synergetic operation of photovoltaic and hydro power stations on a day-ahead energy market. *Energy* **2020**, *212*, 118686, doi:10.1016/j.energy.2020.118686.
18. Halamay, D.A.; Brekken, T.K.A.; Simmons, A.; McArthur, S. Reserve Requirement Impacts of Large-Scale Integration of Wind, Solar, and Ocean Wave Power Generation. *IEEE Transactions on Sustainable Energy* **2011**, *2*, 321–328, doi:10.1109/tste.2011.2114902.
19. Sun, W.; Harrison, G.P. Wind-solar complementarity and effective use of distribution network capacity. *Applied Energy* **2019**, *247*, 89–101, doi:10.1016/j.apenergy.2019.04.042.
20. Kalogeri, C.; Galanis, G.; Spyrou, C.; Diamantis, D.; Baladima, F.; Koukoula, M.; Kallos, G. Assessing the European offshore wind and wave energy resource for combined exploitation. *Renewable Energy* **2017**, *101*, 244–264, doi:10.1016/J.RENENE.2016.08.010.
21. Gideon, R.A.; Bou-Zeid, E. Collocating offshore wind and wave generators to reduce power output variability: A Multi-site analysis. *Renewable Energy* **2021**, *163*, 1548–1559, doi:10.1016/j.renene.2020.09.047.
22. Rusu, E.; Onea, F. A parallel evaluation of the wind and wave energy resources along the Latin American and European coastal environments. *Renewable Energy* **2019**, *143*, 1594–1607, doi:10.1016/j.renene.2019.05.117.
23. Colmenar-Santos, A.; Reino-Rio, C.; Borge-Diez, D.; Collado-Fernández, E. Distributed generation: A review of factors that can contribute most to achieve a scenario of DG units embedded in the new distribution networks. *Renewable and Sustainable Energy Reviews* **2016**, *59*, 1130–1148, doi:10.1016/j.rser.2016.01.023.
24. Kakran, S.; Chanana, S. Smart operations of smart grids integrated with distributed generation: A review. *Renewable and Sustainable Energy Reviews* **2018**, *81*, 524–535, doi:10.1016/j.rser.2017.07.045.
25. Gururaj, M.V.; Padhy, N.P. An Improvized Coordinated Voltage Control Scheme for Better Utilization of Regulating Devices During Various Operating Conditions of a Distribution System. *IEEE Systems Journal* **2019**, 1–10, doi:10.1109/jsyst.2019.2959407.
26. Sansawatt, T.; Ochoa, L.F.; Harrison, G.P. Smart Decentralized Control of DG for Voltage and Thermal Constraint Management. *IEEE Transactions on Power Systems* **2012**, *27*, 1637–1645, doi:10.1109/TPWRS.2012.2186470.
27. Tang, Z.; Hill, D.J.; Liu, T. Distributed Coordinated Reactive Power Control for Voltage Regulation in Distribution Networks. *IEEE Transactions on Smart Grid* **2020**, 1–1, doi:10.1109/tsg.2020.3018633.
28. Džamarija, M.; Keane, A. Autonomous Curtailment Control n Distributed Generation Planning. *IEEE Transactions on Smart Grid* **2016**, *7*, 1337–1345, doi:10.1109/TSG.2015.2427378.
29. Li, J.; Xu, Z.; Zhao, J.; Zhang, C. Distributed Online Voltage Control in Active Distribution Networks Considering PV Curtailment. *IEEE Transactions on Industrial Informatics* **2019**, *15*, 5519–5530, doi:10.1109/TII.2019.2903888.
30. Kane, L.; Ault, G.W. Evaluation of Wind Power Curtailment in Active Network Management Schemes. *IEEE Trans. Power Syst.* **2015**, *30*, 672–679, doi:10.1109/TPWRS.2014.2336862.
31. Franco, J.F.; Ochoa, L.F.; Romero, R. AC OPF for smart distribution networks: An efficient and robust quadratic approach. *IEEE Transactions on Smart Grid* **2018**, *9*, 4613–4623, doi:10.1109/TSG.2017.2665559.
32. Gill, S.; Kockar, I.; Ault, G.W. Dynamic Optimal Power Flow for Active Distribution Networks. *IEEE Transactions on Power Systems* **2014**, *29*, 121–131, doi:10.1109/TPWRS.2013.2279263.
33. Robertson, J.G.; Harrison, G.P.; Wallace, A.R. OPF Techniques for Real-Time Active Management of

Distribution Networks. *IEEE Trans. Power Syst.* **2017**, *32*, 3529–3537, doi:10.1109/tpwrs.2016.2624985.

34. Ochoa, L.F.; Dent, C.J.; Harrison, G.P. Distribution Network Capacity Assessment: Variable DG and Active Networks. *IEEE Transactions on Power Systems* **2010**, *25*, 87–95, doi:10.1109/tpwrs.2009.2031223.
35. Bisschop, J. *AIMMS Optimization Modeling*; Lulu. com, 2018; ISBN 9781847539120.
36. Hersbach, H.; Bell, B.; Berrisford, P.; Hirahara, S.; Horányi, A.; Muñoz-Sabater, J.; Nicolas, J.; Peubey, C.; Radu, R.; Schepers, D.; et al. The ERA5 global reanalysis. *Quarterly Journal of the Royal Meteorological Society* **2020**, *146*, 1999–2049, doi:10.1002/qj.3803.
37. Copernicus - Marine environment monitoring service Available online: https://marine.copernicus.eu/ (accessed on Jan 15, 2020).
38. ABPmer Atlas of uk marine renewable energy resources. *Technical Report No. R1432* **2008**.
39. Douglas, C.A.; Harrison, G.P.; Chick, J.P. Life cycle assessment of the Seagen marine current turbine. *Proceedings of the Institution of Mechanical Engineers, Part M: Journal of Engineering for the Maritime Environment* **2008**, *222*, 1–12, doi:10.1243/14750902JEME94.
40. Boheme, T.; Taylor, J.; Wallace, A.R.; Bialaek, J. *Matching renewable electricity generation with demand*; Scottish Executive: Edinburgh, 2006;
41. Gordon Edge, Gareth Davies, M.C. *Wave and tidal energy: state of the industry*; 2018;
42. Kalogeri, C.; Galanis, G.; Spyrou, C.; Diamantis, D.; Baladima, F.; Koukoula, M.; Kallos, G. Assessing the European offshore wind and wave energy resource for combined exploitation. *Renewable Energy* **2017**, *101*, 244–264, doi:10.1016/j.renene.2016.08.010.
43. Keane, A.; Ochoa, L.F.; Vittal, E.; Dent, C.J.; Harrison, G.P. Enhanced utilization of voltage control resources with distributed generation. *IEEE Transactions on Power Systems* **2011**, *26*, 252–260, doi:10.1109/TPWRS.2009.2037635.
44. Ochoa, L.F.; Keane, A.; Dent, C.; Harrison, G.P. Applying active network management schemes to an Irish distribution network for wind power maximisation. *IET Conference Publications* **2009**, 890–890, doi:10.1049/cp.2009.1052.